Progress In Electromagnetics Research, PIER 53, 299–318, 2005

T-MATRIX ANALYSIS OF MULTIPLE SCATTERING FROM PARALLEL SEMI-CIRCULAR CHANNELS FILLED WITH CHIRAL MEDIA IN A CONDUCTING PLANE

Y. J. Zhang, A. Bauer, and E. P. Li

Computational Electromagnetics and Electronics
Institute of High Performance Computing
Singapore 117528

Abstract—The T-matrix method is used to model semicircular channels filled with chiral materials in a conducting plane. The coupling of both TM and TE polarizations is represented explicitly. Addition theorems in half space are derived and used to take account of the multiple scattering of parallel channels. The boundary conditions are checked for chiral channels to verify the algorithm proposed. Co- and cross-polarization effects of chiral materials are investigated by varying several physical and geometrical parameters of the parallel channels.

1. INTRODUCTION

Scattering from a semicircular channel is a typical boundary value problem (BVP) in electromagnetics. Many authors have utilized the dual-series solution for the radar cross section (RCS) analysis of a single channel or the one loaded by dielectric cylinders [1–7]. In dual-series solution, the fields are expanded in terms of cylindrical harmonics and boundary conditions are enforced to obtain the expansion coefficients. Recently, the authors in [8] extended the solution to two semicircular channels using the addition theorems in half space. However, only TM polarization is considered.

Generally, the dual-series solution belongs to the mode matching method which has been widely used in modeling the discontinuities in waveguides. The mode matching method could provide very accurate solution efficiently. However, it will become very cumbersome when dealing with complex channel structures. To overcome this drawback, the authors have proposed a novel method which combines T-matrix and microwave network approaches [9]. The introduction of the T-matrix for a semicircular channel greatly simplifies the analysis procedure and thus, very complex channel structures could be handled readily. On the other hand, scattering from channels filled with one kind of novel medium becomes an interesting research topic. For example, P. L. E. Uslenghi investigated a slotted semielliptical channel filled with isorefractive material [10].

In this paper, we extend the T-matrix solution into scattering of parallel channels filled with chiral media. The chiral medium is a special bi-isotropic material which has been continuously studied in this decade [11–13]. It is well known that a linear polarization wave propagating in a chiral material undergoes a rotation of its polarization. This means TM and TE waves are coupled together and thus, could not be analyzed separately. This introduces additional difficulties in analysis. Here, we first derive the T-matrix of a single channel filled with a chiral medium. This T-matrix includes the coupling effects explicitly. Then addition theorems in half space are used to consider the multiple scattering of several channels. All the formulas are expressed in matrix form to ease the implementation. Section 2 will derive the T-matrix of a single chiral-filled channel. In Section 3, multiple scattering of parallel channels are discussed with the aid of addition theorems in half space. Validation and numerical examples are provided in Section 4 followed by a short conclusion.

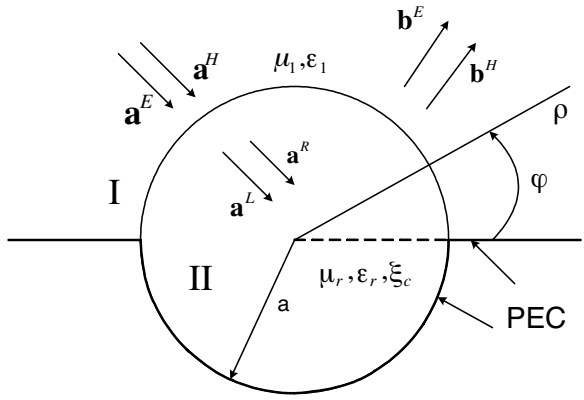

Figure 1. Cross section of a single channel filled with a chiral medium.

2. T-MATRIX OF A SINGLE SEMICIRCULAR CHANNEL FILLED WITH CHIRAL MATERIAL

Let us first consider a semicircular channel filled with a chiral medium in a ground plane as shown in Fig. 1. The channel locates in an isotropic medium with the relative permittivity ε_1 and permeability μ_1 (region I). The radius of the channel is denoted as and the chiral material is characterized as $(\mu_r, \varepsilon_r, \xi_r)$ which represents relative permeability, permittivity and chirality admittance, respectively (region II). These parameters describe the constitutive relations of the chiral medium as (time factor $e^{j\omega t}$ is assumed throughout the paper):

$$\boldsymbol{D} = \varepsilon_r \varepsilon_0 \boldsymbol{E} - j\xi_c \boldsymbol{B} \tag{1}$$

$$\boldsymbol{H} = \frac{1}{\mu_r \mu_0} \boldsymbol{B} - j\xi_c \boldsymbol{E} \tag{2}$$

It is well known that a chiral medium supports both right and left circular polarized waves with two different wave numbers k_R and k_L respectively, given by

$$k_R = k_0 \sqrt{\mu_r \varepsilon_r} \left(\sqrt{1 + \chi^2} + \chi \right) \tag{3}$$

$$k_L = k_0 \sqrt{\mu_r \varepsilon_r} \left(\sqrt{1 + \chi^2} - \chi \right) \tag{4}$$

where the chirality parameter $\chi = \sqrt{\mu_r / \varepsilon_r} \eta_0 \xi_c$, is a dimensionless value and $\eta_0 = 120\pi$ ohms is the wave impedance of free space.

Since the TM and TE waves are coupled together in the chiral medium, the corresponding electric and magnetic components in region I could be written as follows:

$$E_z^I = \sum_{n=1}^{\infty} \left[a_n^E J_n(k_I\rho)\sin n\varphi + b_n^E H_n^{(2)}(k_I\rho)\sin n\varphi \right] \tag{5a}$$

$$H_z^I = \sum_{n=0}^{\infty} \left[a_n^H J_n(k_I\rho)\cos n\varphi + b_n^H H_n^{(2)}(k_I\rho)\cos n\varphi \right] \tag{5b}$$

$$E_\varphi^I = j\eta_0\sqrt{\frac{\mu_1}{\varepsilon_1}} \sum_{n=0}^{\infty} \left[a_n^H J_n'(k_I\rho)\cos n\varphi + b_n^H H_n^{(2)'}(k_I\rho)\cos n\varphi \right] \tag{5c}$$

$$H_\varphi^I = \frac{1}{j\eta_0}\sqrt{\frac{\varepsilon_1}{\mu_1}} \sum_{n=0}^{\infty} \left[a_n^E J_n'(k_I\rho)\sin n\varphi + b_n^E H_n^{(2)'}(k_I\rho)\sin n\varphi \right] \tag{5d}$$

where $J_n(\cdot)$ and $H_n^{(2)}(\cdot)$ are n-th order of the Bessel function and the second kind of Hankel function, respectively. From Eqs. (5a)–(5d), one can observe that the expansion vectors $\boldsymbol{a}^E$, $\boldsymbol{a}^H$ and $\boldsymbol{b}^E$, $\boldsymbol{b}^H$ could be viewed as the incident and scattering field respectively, for either TM or TE waves. On the other hand, in region II, the corresponding electric and magnetic fields are expressed as [12]:

$$\begin{bmatrix} E_z \\ H_z \end{bmatrix} = \begin{bmatrix} 1 & 1 \\ j\eta_c^{-1} & -j\eta_c^{-1} \end{bmatrix} \begin{bmatrix} R_z \\ -L_z \end{bmatrix} \tag{6}$$

$$\begin{bmatrix} E_\varphi \\ H_\varphi \end{bmatrix} = -\begin{bmatrix} 1 & 1 \\ j\eta_c^{-1} & -j\eta_c^{-1} \end{bmatrix} \begin{bmatrix} k_R^{-1}\partial_p R_z \\ k_L^{-1}\partial_p L_z \end{bmatrix} \tag{7}$$

where ∂_ρ is the partial derivative with the radius ρ and the chiral wave impedance η_c is defined as

$$\eta_c = \frac{\sqrt{\mu_r/\varepsilon_r}\eta_0}{\sqrt{1+\chi^2}} \tag{8}$$

In Eqs. (6) and (7), the auxiliary functions R_z and L_z satisfy 2D Helmholtz equation and are pertaining to the right and left circular polarized waves, respectively. Since there is no irregular inclusions in region II, R_z and L_z are expanded with the Bessel functions as

$$R_z = \sum_{n=-\infty}^{\infty} a_n^R J_n(k_R\rho)e^{jn\varphi} \tag{9}$$

$$L_z = \sum_{n=-\infty}^{\infty} a_n^L J_n(k_L\rho)e^{jn\varphi} \tag{10}$$

where coefficient vector $\boldsymbol{a}^R$ and $\boldsymbol{a}^L$ represent the corresponding right and left circular polarized waves, respectively. Substituting (9) and (10) into (6) and (7), we could express the relavant field components in region II as:

$$E_z^{II} = \sum_{n=-\infty}^{\infty} \left[a_n^R J_n(k_R\rho)e^{jn\varphi} - a_n^L J_n(k_L\rho)e^{jn\varphi} \right] \tag{11a}$$

$$H_z^{II} = j\eta_c^{-1} \sum_{n=-\infty}^{\infty} \left[a_n^R J_n(k_R\rho)e^{jn\varphi} + a_n^L J_n(k_L\rho)e^{jn\varphi} \right] \tag{11b}$$

$$E_\varphi^{II} = -\sum_{n=-\infty}^{\infty} \left[a_n^R J_n'(k_R\rho)e^{jn\varphi} + a_n^L J_n'(k_L\rho)e^{jn\varphi} \right] \tag{11c}$$

$$H_\varphi^{II} = -j\eta_c^{-1} \sum_{n=-\infty}^{\infty} \left[a_n^R J_n'(k_R\rho)e^{jn\varphi} + a_n^L J_n'(k_L\rho)e^{jn\varphi} \right] \tag{11d}$$

The objective in this section is to derive T-matrix relating outward waves $\boldsymbol{b}^E$ and $\boldsymbol{b}^H$ to inward excitations $\boldsymbol{a}^E$ and $\boldsymbol{a}^H$ as

$$\begin{bmatrix} \boldsymbol{b}^E \\ \boldsymbol{b}^H \end{bmatrix} = \begin{bmatrix} \boldsymbol{T}^{ee} & \boldsymbol{T}^{eh} \\ \boldsymbol{T}^{he} & \boldsymbol{T}^{hh} \end{bmatrix} \begin{bmatrix} \boldsymbol{a}^E \\ \boldsymbol{a}^H \end{bmatrix} \tag{12}$$

where the matrices $\boldsymbol{T}^{ee}$, $\boldsymbol{T}^{hh}$ are the T-matrices for co-polarization components while $\boldsymbol{T}^{eh}$, $\boldsymbol{T}^{he}$, represent the cross-polarization effects of the chiral medium. Obviously, $\boldsymbol{T}^{eh}$ and $\boldsymbol{T}^{he}$ should vanish in case of the isotropic-filled channels. Here, we enforce the continuous boundary conditions of the tangential electric and magnetic fields on $\rho = a$ as following:

$$E_z^{II} = \begin{cases} E_z^I & \varphi \in [0,\pi] \\ 0 & \varphi \in [\pi, 2\pi] \end{cases} \tag{13a}$$

$$E_\varphi^{II} = \begin{cases} E_\varphi^I & \varphi \in [0,\pi] \\ 0 & \varphi \in [\pi, 2\pi] \end{cases} \tag{13b}$$

$$H_z^{II} = H_z^I \quad \varphi \in [0,\pi] \tag{13c}$$

$$H_\varphi^{II} = H_\varphi^I \quad \varphi \in [0,\pi] \tag{13d}$$

Substituting (5a–d) and (11a–d) into (13a–d), yield

$$\sum_{n=-Q}^{Q} \begin{bmatrix} a_n^R J_n(k_R a)e^{jn\varphi} - \\ a_n^L J_n(k_L a)e^{jn\varphi} \end{bmatrix} = \begin{cases} \sum_{n=1}^{N_E} \begin{bmatrix} a_n^E J_n(k_I a)\sin n\varphi + \\ b_n^E H_n^{(2)}(k_I a)\sin n\varphi \end{bmatrix} & \varphi \in [0,\pi] \\ 0 & \varphi \in [\pi, 2\pi] \end{cases} \tag{14a}$$

$$\sum_{n=-Q}^{Q}\begin{bmatrix} a_n^R J_n'(k_R a)e^{jn\varphi}+ \\ a_n^L J_n'(k_L a)e^{jn\varphi} \end{bmatrix} = \begin{cases} \dfrac{\eta_0}{j}\sqrt{\dfrac{\mu_1}{\varepsilon_1}}\displaystyle\sum_{n=0}^{N_H}\begin{bmatrix} a_n^H J_n'(k_I a)\cos n\varphi+ \\ b_n^H H_n^{(2)'}(k_I a)\cos n\varphi \end{bmatrix} & \\ \qquad\qquad\qquad\qquad \varphi\in[0,\pi] & \\ 0 \qquad\qquad\qquad\qquad \varphi\in[\pi,2\pi] & \end{cases} \tag{14b}$$

$$j\eta_c^{-1}\sum_{n=-Q}^{Q}\begin{bmatrix} a_n^R J_n(k_R a)e^{jn\varphi}+ \\ a_n^L J_n(k_L a)e^{jn\varphi} \end{bmatrix} = \sum_{n=0}^{N_H}\begin{bmatrix} a_n^H J_n(k_I a)\cos n\varphi+ \\ b_n^H H_n^{(2)}(k_I a)\cos n\varphi \end{bmatrix} \quad \varphi\in[0,\pi] \tag{14c}$$

$$\eta_c^{-1}\sum_{n=-Q}^{Q}\begin{bmatrix} a_n^R J_n'(k_R a)e^{jn\varphi}- \\ a_n^L J_n'(k_L a)e^{jn\varphi} \end{bmatrix} = \begin{cases} \eta_0^{-1}\sqrt{\dfrac{\varepsilon_1}{\mu_1}}\displaystyle\sum_{n=1}^{N_E}\begin{bmatrix} a_n^E J_n'(k_I a)\sin n\varphi+ \\ b_n^E H_n^{(2)'}(k_I a)\sin n\varphi \end{bmatrix} & \\ \qquad\qquad\qquad\qquad \varphi\in[0,\pi] & \\ 0 \qquad\qquad\qquad\qquad \varphi\in[\pi,2\pi] & \end{cases} \tag{14d}$$

Notice that the infinite coefficient vectors $\boldsymbol{a}^E(\boldsymbol{b}^E)$, $\boldsymbol{a}^H(\boldsymbol{b}^H)$, and $\boldsymbol{a}^R(\boldsymbol{a}^L)$ have been truncated into finite vectors with N_E, N_H+1 and $2Q+1$ elements, respectively. By multiplying both sides of Eqs. (14a) and (14b) with $e^{-jm\varphi}$ and integrating φ in $[0,2\pi]$; and similarly, multiplying Eq. (14c) with $\cos m\varphi$, Eq. (14d) with $\sin m\varphi$, and integrating φ in $[0,\pi]$; then we have

$$\boldsymbol{J}_R\boldsymbol{a}^R - \boldsymbol{J}_L\boldsymbol{a}^L = \boldsymbol{J}_I\boldsymbol{a}^E + \boldsymbol{H}_I\boldsymbol{b}^E \tag{15a}$$

$$\boldsymbol{J}_R'\boldsymbol{a}^R + \boldsymbol{J}_L'\boldsymbol{a}^L = \boldsymbol{J}_I'\boldsymbol{a}^H + \boldsymbol{H}_I'\boldsymbol{b}^H \tag{15b}$$

$$\boldsymbol{J}_R^C\boldsymbol{a}^R + \boldsymbol{J}_L^C\boldsymbol{a}^L = \boldsymbol{J}_I^C\boldsymbol{a}^H + \boldsymbol{H}_I^C\boldsymbol{b}^H \tag{15c}$$

$$\boldsymbol{J}_R^S\boldsymbol{a}^R - \boldsymbol{J}_L^S\boldsymbol{a}^L = \boldsymbol{J}_I^S\boldsymbol{a}^E + \boldsymbol{H}_I^S\boldsymbol{b}^E \tag{15d}$$

The elements of matrices in (15a–d) could be evaluated analytically and listed in the Appendix. Eqs. (15a–d) is further written as following equations:

$$\begin{bmatrix} \boldsymbol{J}_R & -\boldsymbol{J}_L \\ \boldsymbol{J}_R' & \boldsymbol{J}_L' \end{bmatrix}\begin{bmatrix} \boldsymbol{a}^R \\ \boldsymbol{a}^L \end{bmatrix} = \begin{bmatrix} \boldsymbol{H}_I & 0 \\ 0 & \boldsymbol{H}_I' \end{bmatrix}\begin{bmatrix} \boldsymbol{b}^E \\ \boldsymbol{b}^H \end{bmatrix} + \begin{bmatrix} \boldsymbol{J}_I & 0 \\ 0 & \boldsymbol{J}_I' \end{bmatrix}\begin{bmatrix} \boldsymbol{a}^E \\ \boldsymbol{a}^H \end{bmatrix} \tag{16}$$

$$\begin{bmatrix} \boldsymbol{J}_R^S & -\boldsymbol{J}_L^S \\ \boldsymbol{J}_R^C & \boldsymbol{J}_L^C \end{bmatrix}\begin{bmatrix} \boldsymbol{a}^R \\ \boldsymbol{a}^L \end{bmatrix} = \begin{bmatrix} \boldsymbol{H}_I^S & 0 \\ 0 & \boldsymbol{H}_I^C \end{bmatrix}\begin{bmatrix} \boldsymbol{b}^E \\ \boldsymbol{b}^H \end{bmatrix} + \begin{bmatrix} \boldsymbol{J}_I^S & 0 \\ 0 & \boldsymbol{J}_I^C \end{bmatrix}\begin{bmatrix} \boldsymbol{a}^E \\ \boldsymbol{a}^H \end{bmatrix} \tag{17}$$

From Eqs. (12), (16) and (17), yields

$$\begin{bmatrix} \boldsymbol{T}^{ee} & \boldsymbol{T}^{eh} \\ \boldsymbol{T}^{he} & \boldsymbol{T}^{hh} \end{bmatrix} = \left\{ \begin{bmatrix} \boldsymbol{H}_I^S & 0 \\ 0 & \boldsymbol{H}_I^C \end{bmatrix} - \begin{bmatrix} \boldsymbol{J}_R^S & -\boldsymbol{J}_L^S \\ \boldsymbol{J}_R^C & \boldsymbol{J}_L^C \end{bmatrix} \begin{bmatrix} \boldsymbol{J}_R & -\boldsymbol{J}_L \\ \boldsymbol{J}'_R & \boldsymbol{J}'_L \end{bmatrix}^{-1} \begin{bmatrix} \boldsymbol{H}_I & 0 \\ 0 & \boldsymbol{H}'_I \end{bmatrix} \right\}^{-1} \left\{ \begin{bmatrix} \boldsymbol{J}_R^S & -\boldsymbol{J}_L^S \\ \boldsymbol{J}_R^C & \boldsymbol{J}_L^C \end{bmatrix} \begin{bmatrix} \boldsymbol{J}_R & -\boldsymbol{J}_L \\ \boldsymbol{J}'_R & \boldsymbol{J}'_L \end{bmatrix}^{-1} \begin{bmatrix} \boldsymbol{J}_I & 0 \\ 0 & \boldsymbol{J}'_I \end{bmatrix} - \begin{bmatrix} \boldsymbol{J}_I^S & 0 \\ 0 & \boldsymbol{J}_I^C \end{bmatrix} \right\} \quad (18)$$

It is worth to note that the matrices $\boldsymbol{T}^{ee}$, $\boldsymbol{T}^{eh}$, $\boldsymbol{T}^{he}$, $\boldsymbol{T}^{hh}$ are $N_E \times N_E$, $N_E \times (N_H+1)$, $(N_H+1) \times N_E$, $(N_H+1) \times (N_H+1)$ matrices, respectively. The parameters N_E, N_H, Q should be selected carefully to get the convergence of final RCS calculation. In our simulation, we chose N_E, N_H, Q related to the geometrical and electrical parameters as $N_E \approx N_H \approx Q \approx (1.5 \sim 2.0)k_R a$.

3. MULTIPLE SCATTERING FROM PARALLEL CHIRAL-FILLED CHANNELS

To consider the multiple scattering between parallel channels using the T-matrix derived above, a new set of addition theorems in half space could be derived [9] as follows:

$$H_m^{(2)}(k|\boldsymbol{\rho} - \boldsymbol{\rho}_j|) \sin m\varphi_j = \begin{cases} \displaystyle\sum_{n=1}^{\infty} \left\{ \begin{matrix} [J_{n-m}(k\rho_{ji}) - (-1)^m J_{n+m}(k\rho_{ji})] \\ \cos n\varphi_{ji} \cos m\varphi_{ji} \end{matrix} \right\} H_n^{(2)}(k|\boldsymbol{\rho} - \boldsymbol{\rho}_i|) \sin n\varphi_i \\ \qquad\qquad |\boldsymbol{\rho} - \boldsymbol{\rho}_i| > \rho_{ji} \\ \displaystyle\sum_{n=1}^{\infty} \left\{ \begin{matrix} \left[H_{n-m}^{(2)}(k\rho_{ji}) - (-1)^m H_{n+m}^{(2)}(k\rho_{ji})\right] \\ \cos n\varphi_{ji} \cos m\varphi_{ji} \end{matrix} \right\} J_n(k|\boldsymbol{\rho} - \boldsymbol{\rho}_i|) \sin n\varphi_i \\ \qquad\qquad |\boldsymbol{\rho} - \boldsymbol{\rho}_i| < \rho_{ji} \end{cases} \quad (19)$$

$$H_m^{(2)}(k|\boldsymbol{\rho} - \boldsymbol{\rho}_j|) \cos m\varphi_j = \begin{cases} \displaystyle\sum_{n=0}^{\infty} \frac{2-\delta_{n0}}{2} \left\{ \begin{matrix} [J_{n-m}(k\rho_{ji}) + (-1)^m J_{n+m}(k\rho_{ji})] \\ \cos n\varphi_{ji} \cos m\varphi_{ji} \end{matrix} \right\} H_n^{(2)}(k|\boldsymbol{\rho} - \boldsymbol{\rho}_i|) \cos n\varphi_i \\ \qquad\qquad |\boldsymbol{\rho} - \boldsymbol{\rho}_i| > \rho_{ji} \\ \displaystyle\sum_{n=0}^{\infty} \frac{2-\delta_{n0}}{2} \left\{ \begin{matrix} \left[H_{n-m}^{(2)}(k\rho_{ji}) + (-1)^m H_{n+m}^{(2)}(k\rho_{ji})\right] \\ \cos n\varphi_{ji} \cos m\varphi_{ji} \end{matrix} \right\} J_n(k|\boldsymbol{\rho} - \boldsymbol{\rho}_i|) \cos n\varphi_i \\ \qquad\qquad |\boldsymbol{\rho} - \boldsymbol{\rho}_i| < \rho_{ji} \end{cases} \quad (20)$$

$$J_m(k|\boldsymbol{\rho}-\boldsymbol{\rho}_j|)\sin m\varphi_j = \sum_{n=1}^{\infty}\left\{\begin{array}{l}[J_{n-m}(k\rho_{ji})-(-1)^m J_{n+m}(k\rho_{ji})]\\ \cos n\varphi_{ji}\cos m\varphi_{ji}\end{array}\right\} J_n(k|\boldsymbol{\rho}-\boldsymbol{\rho}_i|)\sin n\varphi_i \quad (21)$$

$$J_m(k|\boldsymbol{\rho}-\boldsymbol{\rho}_j|)\cos m\varphi_j = \sum_{n=0}^{\infty}\frac{2-\delta_{n0}}{2}\left\{\begin{array}{l}[J_{n-m}(k\rho_{ji})+(-1)^m J_{n+m}(k\rho_{ji})]\\ \cos n\varphi_{ji}\cos m\varphi_{ji}\end{array}\right\} J_n(k|\boldsymbol{\rho}-\boldsymbol{\rho}_i|)\cos n\varphi_i \quad (22)$$

The geometric meaning of the parameters in (19)–(22) is shown in Fig. 2. It should stress that $\varphi_{ji} = \arg(\boldsymbol{\rho}_j - \boldsymbol{\rho}_i)$ which means if $\boldsymbol{\rho}_j$ lies on the right of $\boldsymbol{\rho}_i$, then $\varphi_{ji} = 0$ while $\boldsymbol{\rho}_j$ lies on the left of $\boldsymbol{\rho}_i$, $\varphi_{ji} = \pi$.

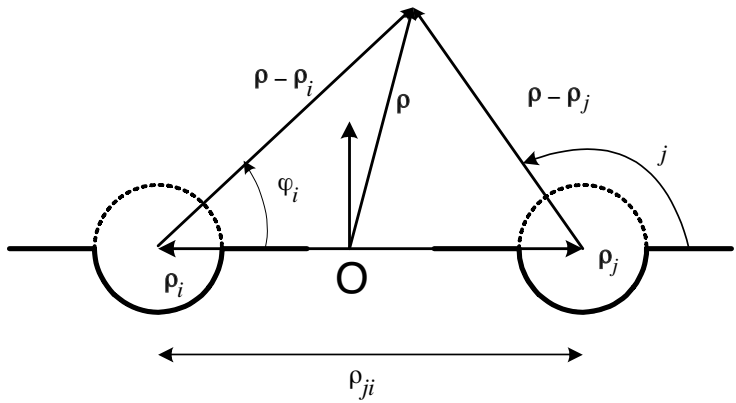

Figure 2. Coordinate system transform in two semicircular channels.

We assume that there are totally M channels and for each channel, the scattering field in its local coordinates are represented as $\boldsymbol{b}_i^E$ and $\boldsymbol{b}_i^H$, $i = 1, 2, \ldots, M$. Then we have following equations:

$$\boldsymbol{b}_i^E = \boldsymbol{T}_i^{ee}\left(\boldsymbol{\beta}_{i0}^E\boldsymbol{a}_0^E + \sum_{\substack{j=1\\ j\neq i}}^{M}\boldsymbol{\alpha}_{ij}^E\boldsymbol{b}_j^E\right) + \boldsymbol{T}_i^{eh}\left(\boldsymbol{\beta}_{i0}^H\boldsymbol{a}_0^H + \sum_{\substack{j=1\\ j\neq i}}^{M}\boldsymbol{\alpha}_{ij}^H\boldsymbol{b}_j^H\right) \quad (23)$$

$$\boldsymbol{b}_i^H = \boldsymbol{T}_i^{he}\left(\boldsymbol{\beta}_{i0}^E\boldsymbol{a}_0^E + \sum_{\substack{j=1\\ j\neq i}}^{M}\boldsymbol{\alpha}_{ij}^E\boldsymbol{b}_j^E\right) + \boldsymbol{T}_i^{hh}\left(\boldsymbol{\beta}_{i0}^H\boldsymbol{a}_0^H + \sum_{\substack{j=1\\ j\neq i}}^{M}\boldsymbol{\alpha}_{ij}^H\boldsymbol{b}_j^H\right) \quad (24)$$

where $\boldsymbol{T}_i^{pq}$, $p, q = e, h$ are sub-matrices of the T-matrix of i-th channel;

the matrix $\boldsymbol{\beta}_{i0}^{p},\ p=E,H$ denotes the transform of incident wave from global origin to the center of i-th channel, whose elements are evaluated as:

$$\boldsymbol{\beta}_{i0}^{p}(m,n)=\begin{cases}\left[\begin{array}{l}J_{m-n}(k_I\rho_i)-\\(-1)^n J_{m+n}(k_I\rho_i)\end{array}\right]\cos n\varphi_{ji}\cos m\varphi_{ji} \\ \qquad\qquad m,n=1,2,\ldots \quad p=E \\ \dfrac{2-\delta_{m0}}{2}\left[\begin{array}{l}J_{m-n}(k_I\rho_i)+\\(-1)^n J_{m+n}(k_I\rho_i)\end{array}\right]\cos n\varphi_{ji}\cos m\varphi_{ji} \\ \qquad\qquad m,n=0,1,\ldots \quad p=H\end{cases} \tag{25}$$

and the matrix $\boldsymbol{\alpha}_{ij}^{p},\ p=E,H$ stands for the transform of the scattering wave in j-th channel to the incident wave in i-th channel, and its elements are obtained by

$$\boldsymbol{\alpha}_{ij}^{p}(m,n)=\begin{cases}\left[\begin{array}{l}H_{m-n}^{(2)}(k_I\rho_{ij})-\\(-1)^n H_{m+n}^{(2)}(k_I\rho_{ij})\end{array}\right]\cos n\varphi_{ji}\cos m\varphi_{ji} \\ \qquad\qquad m,n=1,2,\ldots \quad p=E \\ \dfrac{2-\delta_{m0}}{2}\left[\begin{array}{l}H_{m-n}^{(2)}(k_I\rho_{ij})+\\(-1)^n H_{m+n}^{(2)}(k_I\rho_{ij})\end{array}\right]\cos n\varphi_{ji}\cos m\varphi_{ji} \\ \qquad\qquad m,n=0,1,\ldots \quad p=H\end{cases} \tag{26}$$

In (23) and (24), $\boldsymbol{a}_0^E$ and $\boldsymbol{a}_0^H$ stand for the incident TM and TE waves in global coordinate systems. The holding of the Eqs. (23) and (24) is due to the fact that for the i-th channel, the illuminating sources consist of both TM and TE waves and for each polarization, it contains both the incident waves outside of all channels and the scattering waves from other channels.

Combining all the equations (23) and (24) for all channels, we have

$$\begin{bmatrix}\boldsymbol{b}^E\\ \boldsymbol{b}^H\end{bmatrix}=\begin{bmatrix}\boldsymbol{T}^{EE} & \boldsymbol{T}^{EH}\\ \boldsymbol{T}^{HE} & \boldsymbol{T}^{HH}\end{bmatrix}\left\{\begin{bmatrix}\boldsymbol{\beta}_1^E & 0\\ 0 & \boldsymbol{\beta}_1^H\end{bmatrix}\begin{bmatrix}\boldsymbol{a}_0^E\\ \boldsymbol{a}_0^H\end{bmatrix}+\begin{bmatrix}\boldsymbol{\alpha}^E & 0\\ 0 & \boldsymbol{\alpha}^H\end{bmatrix}\begin{bmatrix}\boldsymbol{b}^E\\ \boldsymbol{b}^H\end{bmatrix}\right\} \tag{27}$$

The combined matrices involved in Eq. (27) are listed as

$$\boldsymbol{b}^p=\begin{bmatrix}\boldsymbol{b}_1^p\\ \boldsymbol{b}_2^p\\ \vdots\\ \boldsymbol{b}_M^p\end{bmatrix}\quad \boldsymbol{\beta}_1^p=\begin{bmatrix}\boldsymbol{\beta}_{10}^p\\ \boldsymbol{\beta}_{20}^p\\ \vdots\\ \boldsymbol{\beta}_{M0}^p\end{bmatrix}\quad \boldsymbol{\alpha}^p=\begin{bmatrix}0 & \boldsymbol{\alpha}_{12}^p & \cdots & \boldsymbol{\alpha}_{1M}^p\\ \boldsymbol{\alpha}_{21}^p & 0 & \cdots & \boldsymbol{\alpha}_{2M}^p\\ \vdots & \vdots & \ddots & \vdots\\ \boldsymbol{\alpha}_{M1}^p & \boldsymbol{\alpha}_{M2}^p & \cdots & 0\end{bmatrix} \tag{28}$$

where $p = E$ for TM or TE waves and

$$\boldsymbol{T}^{PQ} = \begin{bmatrix} \boldsymbol{T}_1^{pq} & 0 & \cdots & 0 \\ 0 & \boldsymbol{T}_2^{pq} & \cdots & 0 \\ \vdots & \vdots & \ddots & \vdots \\ 0 & 0 & \cdots & \boldsymbol{T}_M^{pq} \end{bmatrix} \quad p, q = e, h;\ P, Q = E, H \tag{29}$$

The unknowns $\boldsymbol{b}^E$ and $\boldsymbol{b}^H$ in Eq. (27) could be solved directly and expressed as:

$$\begin{bmatrix} \boldsymbol{b}^E \\ \boldsymbol{b}^H \end{bmatrix} = \left\{ \boldsymbol{I} - \begin{bmatrix} \boldsymbol{T}^{EE} & \boldsymbol{T}^{EH} \\ \boldsymbol{T}^{HE} & \boldsymbol{T}^{HH} \end{bmatrix} \begin{bmatrix} \boldsymbol{\alpha}^E & 0 \\ 0 & \boldsymbol{\alpha}^H \end{bmatrix} \right\}^{-1} \begin{bmatrix} \boldsymbol{T}^{EE} & \boldsymbol{T}^{EH} \\ \boldsymbol{T}^{HE} & \boldsymbol{T}^{HH} \end{bmatrix} \begin{bmatrix} \boldsymbol{\beta}_1^E & 0 \\ 0 & \boldsymbol{\beta}_1^H \end{bmatrix} \begin{bmatrix} \boldsymbol{a}_0^E \\ \boldsymbol{a}_0^H \end{bmatrix} \tag{30}$$

Therefore, the scattering field could be obtained readily as

$$E_z^S(\varphi) = \sum_{i=1}^{M} \sum_{n=1}^{N_E} b_i^E(n) H_m^{(2)}(k_I |\boldsymbol{\rho} - \boldsymbol{\rho}_i|) \sin n\varphi_i \tag{31a}$$

$$H_z^S(\varphi) = \sum_{i=1}^{M} \sum_{n=1}^{N_H} b_i^H(n) H_n^{(2)}(k_I |\boldsymbol{\rho} - \boldsymbol{\rho}_i|) \cos n\varphi_i \tag{31b}$$

Using the large argument approximation of the Hankel functions, the co-polarization echo width of parallel channels is expressed as:

$$\sigma^{EE}(\varphi) = \frac{\dfrac{4}{k_I} \left| \displaystyle\sum_{i=1}^{M} e^{jk\rho_i \cos\varphi} \sum_{n=1}^{N_E} b_i^E(n) j^n \sin n\varphi \right|^2}{|E_z^{inc}|^2} \tag{32a}$$

$$\sigma^{HH}(\varphi) = \frac{\dfrac{4}{k_I} \left| \displaystyle\sum_{i=1}^{M} e^{jk\rho_i \cos\varphi} \sum_{n=0}^{N_H} b_i^H(n) j^n \cos n\varphi \right|^2}{|H_z^{inc}|^2} \tag{32b}$$

The cross-polarization echo width is defined as

$$\sigma^{EH}(\varphi) = \frac{\dfrac{4}{k_I} \left| \displaystyle\sum_{i=1}^{M} e^{jk\rho_i \cos\varphi} \sum_{n=1}^{N_E} b_i^E(n) j^n \sin n\varphi \right|^2}{|\eta_I H_z^{inc}|^2} \tag{32c}$$

$$\sigma^{HE}(\varphi) = \frac{\dfrac{4}{k_I} \left| \displaystyle\sum_{i=1}^{M} e^{jk\rho_i \cos\varphi} \sum_{n=1}^{N_H} b_i^H(n) j^n \cos n\varphi \right|^2}{|E_z^{inc}/\eta_I|^2} \tag{32d}$$

where $\eta_I = \sqrt{\mu_1/\varepsilon_1}\eta_0$, is the wave impedance in region I.

4. NUMERICAL RESULTS AND DISCUSSIONS

To validate the method proposed, all the results in [3] have been reproduced for a single dielectric-filled semicircular channel in case of either TM or TE waves. For the chiral-filled channels, however, to the best of our knowledge, there are no publications to compare with. Therefore, the tangential field components, as shown in Fig. 3, are carefully checked on the boundary of a chiral-filled channel. In this example, a TE polarized wave incident from 45° upon a channel with radius $a = 2.0\lambda$. From Fig. 3(a), it can be seen that the boundary conditions are satisfied very well except the points near $\phi = 0°(360°)$ or $\phi = 180°$. Fig. 3(b) gives the relative discrepancy of electric fields along the boundary. Again, the greater discrepancy occurs at the tips of the channel. The ripples of electric fields in $[0, \pi]$ could be explained as the Gibbs phenomenon in Fourier transform due to the "sharp jumps" of E_z and E_φ along the boundary at the tips. From the equivalent principle, RCS is an average integration of tangential field components. Therefore, the discrepancies between internal and external field components in these tips do not introduce great errors in RCS calculations.

The backscattering from two channels versus the channel radius is shown in Fig. 4. Obviously, the present method agrees very well with the radial mode matching method used in Ref. [8]. This further verified the proposed algorithm.

Fig. 5 gives a schematic illustration of two chiral-filled channels. The discussions of following examples will based on the geometric and electrical parameters shown in Fig. 5. Fig. 6 provides the bistatic co-polarization and cross-polarization scattering from two chiral channels for either TM or TE waves with the incident angle 45°. It can be seen that in this case, the cross-polarization components are stronger than the co-polarization counterparts in some scattering directions. Fig. 7 studies the backscattering versus the separation of two chiral-filled channels. Obviously, scattering amplitudes vary almost periodically with the increase of the separation for each polarization. Finally, we investigate the impact of the chirality admittance on the backscattering of two channels in Fig. 8. It can be seen that the increase of chirality admittance does not inevitably increase the cross-polarization coupling of the channels. Another observation is that for either TM or TE waves, the cross-polarization is quite sensitive to the chirality admittance. This means the slight variation of the chirality could greatly change the scattering pattern of the cross-polarized waves. To the best of

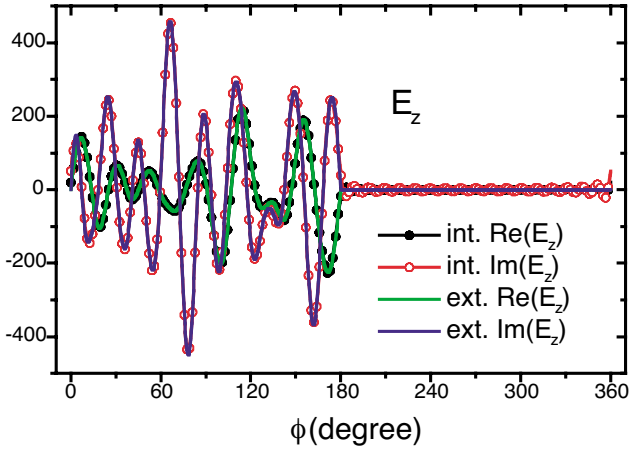

(a)

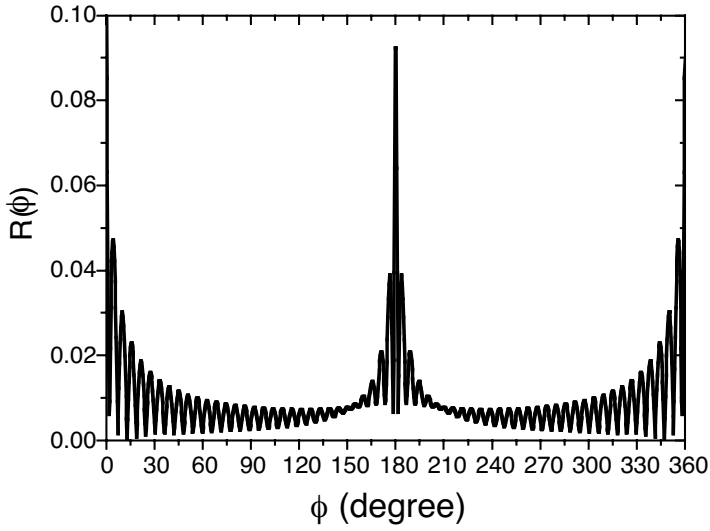

(b)

Figure 3. (a) Real and imaginary parts of external or internal tangential field components on the boundary of a semicircular channel filled with a chiral medium in case of TE wave incidence from angle 45°. (b) The relative discrepancy $R(\varphi) = \frac{|E_z^{ext}(\varphi) - E_z^{\text{int}}(\varphi)|}{\max|E_z^{\text{int}}|)}$ between external and internal electrical fields ($a = 2.0\lambda$, $\mu_r = 1.0$, $\varepsilon_r = 2.0$, $\xi_C = 0.002$).

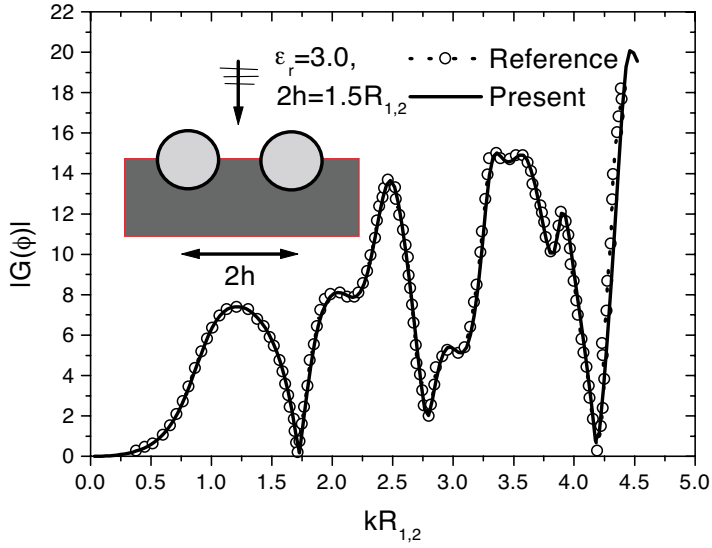

Figure 4. Comparison of the present method with reference [8] (Fig. 2) for backscattering from two dielectric-filled semicircular channels.

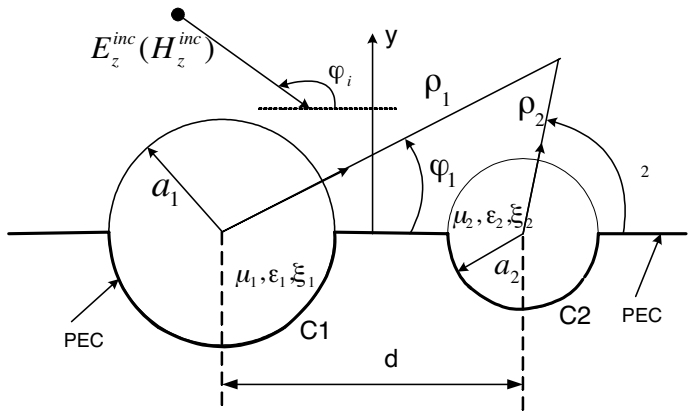

Figure 5. Two parallel chiral-filled semicircular channels.

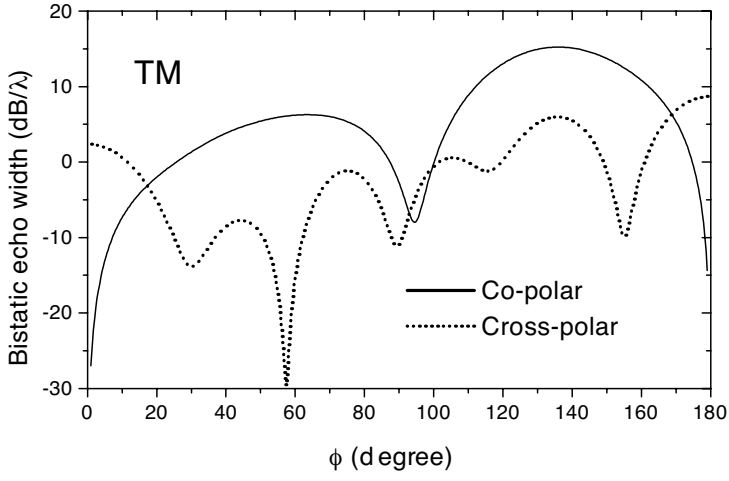

(a)

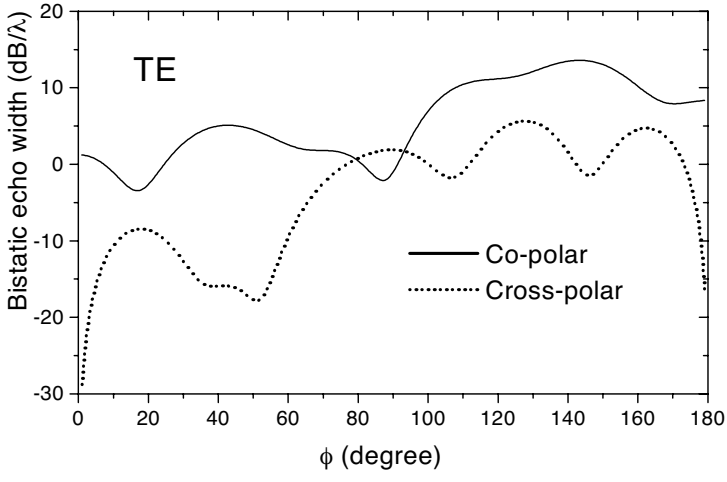

(b)

Figure 6. Co-polar and cross-polar bistatic scattering from two semicircular channels filled with different chiral media. ($\varepsilon_1 = \varepsilon_2 = 2.0,\ \xi_{c1} = 0.005,\ \xi_{c2} = 0.002,\ d = 2.0\lambda,\ a_1 = a_2 = 0.8\lambda,\ \varphi_i = 45^\circ$)

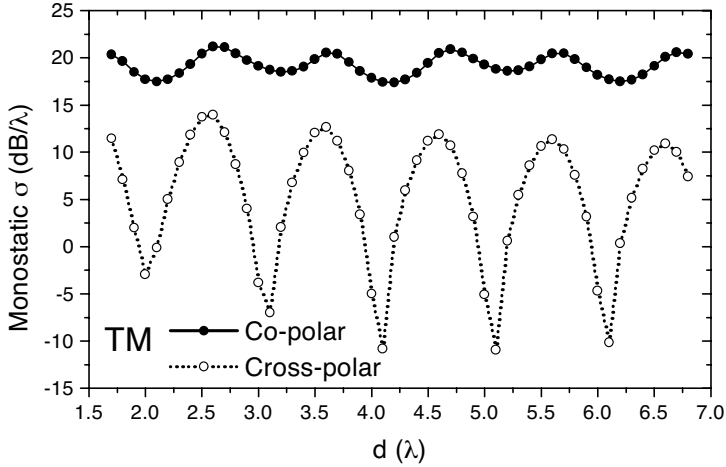

(a)

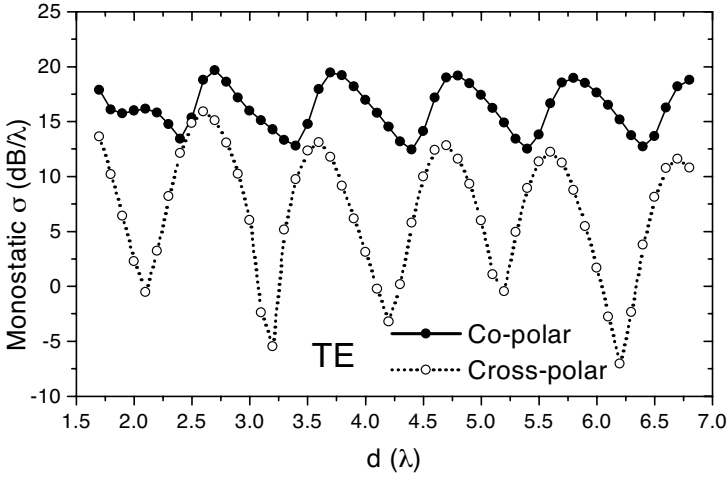

(b)

Figure 7. Backscattering versus the separations of two channels filled with chiral medium. ($\varepsilon_1 = \varepsilon_2 = 2.0$, $\xi_{c1} = \xi_{c2} = 0.005$, $a_1 = a_2 = 0.8\lambda$, $\varphi_i = 90^\circ$)

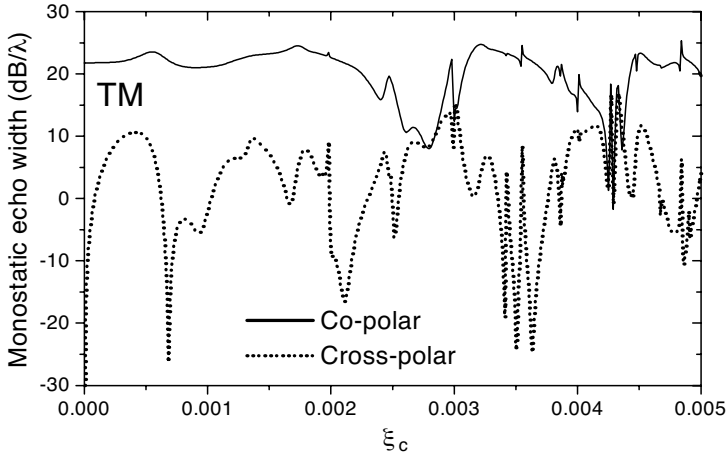

(a)

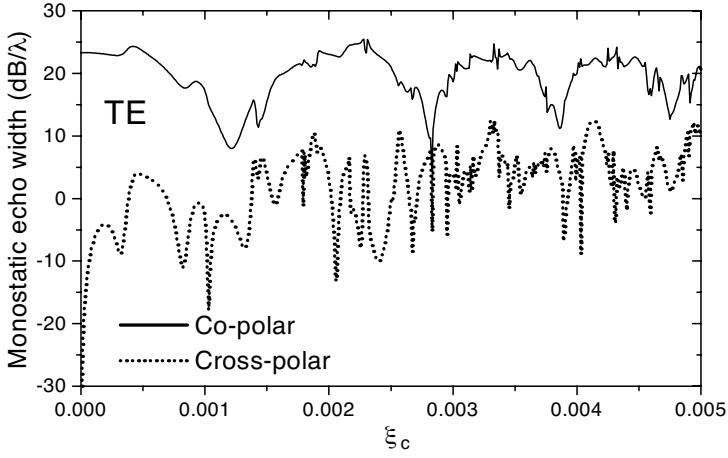

(b)

Figure 8. Backscattering versus the chirality admittance of two chiral-filled channels. ($\varepsilon_1 = \varepsilon_2 = 3.0,\ d = 2.0\lambda,\ a_1 = a_2 = 0.7\lambda,\ \varphi_i = 90^\circ$)

our knowledge, this phenomenon has not been reported before. This sensitivity will surely have some influences on the design of devices containing chiral materials.

5. CONCLUSION

A novel approach is proposed in this paper to simulate the multiple scattering from parallel chiral-filled semicircular channels. In our approach, the T-matrix of a single chiral-filled channel is first derived and then addition theorems in half space are used to take account of the multiple scattering effects among parallel channels. The introduction of T-matrix for chiral-filled channels greatly simplifies the analysis procedure. The effectiveness is validated by either comparing with previous publications or testing the boundary conditions. The impacts of geometric and electrical parameters on the scattering properties of chiral channels are discussed.

APPENDIX A.

For the completeness of the paper, the matrices in (15a–d) and its index range are listed below:

$$\boldsymbol{J}_R(m,n) = 2\pi J_n(k_R a)\delta_{mn} \quad -Q \le m,\ n \le Q \tag{A1}$$

$$\boldsymbol{J}_L(m,n) = 2\pi J_n(k_L a)\delta_{mn} \quad -Q \le m,\ n \le Q \tag{A2}$$

$$\boldsymbol{J}_I(m,n) = J_n(k_I a) f_S(m,n) \quad -Q \le m \le Q,\ 1 \le n \le N_E \tag{A3}$$

$$\boldsymbol{H}_I(m,n) = H_n^{(2)}(k_I a) f_S(m,n) \quad -Q \le m \le Q,\ 1 \le n \le N_E \tag{A4}$$

$$\boldsymbol{J}'_R(m,n) = 2\pi J'_n(k_R a)\delta_{mn} \quad -Q \le m,\ n \le Q \tag{A5}$$

$$\boldsymbol{J}'_L(m,n) = 2\pi J'_n(k_L a)\delta_{mn} \quad -Q \le m,\ n \le Q \tag{A6}$$

$$\boldsymbol{J}'_I(m,n) = \frac{\eta_0}{j}\sqrt{\frac{\mu_1}{\varepsilon_1}} J'_n(k_L a) f_C(m,n) \quad -Q \le m \le Q,\ 0 \le n \le N_H \tag{A7}$$

$$\boldsymbol{H}'_I(m,n) = \frac{\eta_0}{j}\sqrt{\frac{\mu_1}{\varepsilon_1}} H_n^{(2)'}(k_L a) f_C(m,n) \quad -Q \le m \le Q,\ 0 \le n \le N_H \tag{A8}$$

$$\boldsymbol{J}_R^C(m,n) = j\eta_c^{-1} J_n(k_R a) f_C(-n,m) \quad 0 \le m \le N_H,\ -Q \le n \le Q \tag{A9}$$

$$\boldsymbol{J}_L^C(m,n) = j\eta_c^{-1} J_n(k_L a) f_C(-n,m) \quad 0 \le m \le N_H,\ -Q \le n \le Q \tag{A10}$$

$$\boldsymbol{J}_I^C(m,n) = J_n(k_I a) g_C(m,n) \quad 0 \le m,\ n \le N_H \tag{A11}$$

$$\boldsymbol{H}_I^C(m,n) = H_n^{(2)}(k_I a) g_C(m,n) \quad 0 \le m,\ n \le N_H \tag{A12}$$

$$\boldsymbol{J}_R^S(m,n) = \eta_c^{-1} J_n'(k_R a) f_S(-n,m) \quad 1 \le m \le N_E,\ -Q \le n \le Q \tag{A13}$$

$$\boldsymbol{J}_L^S(m,n) = \eta_c^{-1} J_n'(k_L a) f_S(-n,m) \quad 1 \le m \le N_E,\ -Q \le n \le Q \tag{A14}$$

$$\boldsymbol{J}_I^S(m,n) = \eta_0^{-1} \sqrt{\frac{\varepsilon_1}{\mu_1}} J_n'(k_I a) g_S(m,n) \quad 1 \le m,\ n \le N_E \tag{A15}$$

$$\boldsymbol{H}_I^S(m,n) = \eta_0^{-1} \sqrt{\frac{\varepsilon_1}{\mu_1}} H_n^{(2)'}(k_I a) g_S(m,n) \quad 1 \le m,\ n \le N_E \tag{A16}$$

where δ_{mn} is the Kronecker's delta and the functions f_S, f_C, g_S, g_C are defined as:

$$f_S(m,n) = \int_0^\pi e^{-jm\varphi} \sin n\varphi d\varphi \tag{A17}$$

$$f_C(m,n) = \int_0^\pi e^{-jm\varphi} \cos n\varphi d\varphi \tag{A18}$$

$$g_S(m,n) = \int_0^\pi \sin m\varphi \sin n\varphi d\varphi \tag{A19}$$

$$g_C(m,n) = \int_0^\pi \cos m\varphi \cos n\varphi d\varphi \tag{A20}$$

REFERENCES

1. Sachdeva, B. K. and R. K. Hurd, "Scattering by a dielectric-loaded trough in a conducting plane," *J. Appl. Phys.*, Vol. 48, No. 4, 1473–1476, 1977.
2. Senior, T. B. A. and J. L. Volakis, "Scattering from gaps and cracks," *IEEE Trans. Antennas Propagat.*, Vol. 37, 744–750, 1989.
3. Hinders, M. K. and A. D. Yaghjian, "Dual-series solution to scattering from a semicircular channel in a ground plane," *IEEE Microwave and Guided Waves Lett.*, Vol. 1, No. 9, 1991.
4. Park, T. J., H. J. Eom, Y. Yamaguchi, W.-M. Boerner, and S. Kozaki, "TE plane wave scattering from a dielectric-loaded semi-circular trough in a conducting plane," *J. Electromagn. Waves Applicat.*, Vol. 7, No. 2, 234–245, 1993.
5. Ragheb, H. A., "Electromagnetic scattering from a coaxial dielectric circular cylinder loading a semicircular gap in a ground plane," *IEEE Trans. Microwave Theory Tech.*, Vol. 43, No. 6, 1303–1309, 1995.

6. Byun, W. J., J. W. Yu, and N. H. Myung, "TM scattering from hollow and dielectric-filled semielliptic channels with arbitrary eccentricity in a perfectly conducting plane," *IEEE Trans. Microwave Theory Tech.*, Vol. 46, No. 9, 1336–1339, 1998.
7. Tyzhnenko, A. G., "Two-dimensional TE-plane wave scattering by a dielectric-loaded semicircular trough in a ground plane," *Electromagnetics*, Vol. 24, 357–368, 2004.
8. Yu, J. W., W. J. Byun, and N. H. Myung, "Multiple scattering from two dielectric-filled semi-circular channels in a conducting plane: TM case," *IEEE Trans. Antennas Propagat.*, Vol. 50, No. 9, 1250–1253, Sep. 2002.
9. Zhang, Y. J., A. Bauer, and E. P. Li, "A novel coupled T-matrix and microwave network approach for multiple scattering from parallel semicircular channels with eccentric cylindrical inclusions," Accepted by *Progress in Electromagnetics Research*.
10. Uslenghi, P. L. E., "Exact penetration, radiation, and scattering for a slotted semielliptical channel filled with isorefractive material," *IEEE Trans. Antennas propagat.*, Vol. 52, 1473–1480, 2004.
11. Lindell, I. V., A. H. Sihvola, S. A. Tretyakov, and A. J. Viitanen, *Electromagnetic Waves in Chiral and Bi-isotropic Media*, Artech, Norwood, MA, 1994.
12. Kluskens, M. S. and E. H. Newman, "Scattering by a multilayer chiral cylinder," *IEEE Trans. Antennas Propagat.*, Vol. 39, No. 1, 91–96, 1991.
13. Elsherbeni, A. Z., H. A. Sharkawy, and S. F. Mahmoud, "Electromagnetic scattering from a 2-D chiral strip simulated by circular cylinders for uniform and nonuniform chirality distribution," *IEEE Trans. Antennas Propagat.*, Vol. 52, No. 9, 2244–2252, 2004.

Yao Jiang Zhang received B.E. and M.E. degrees in 1991 and 1994 from University of Science & Technology of China, both in Electrical Engineering, Hefei, Anhui, China. In 1999, He received Ph.D. degree in Physical Electronics from Beijing University. From Sept. 1999 to July 2001, he was with Tsinghua University, Beijing, China, as a Postdoctoral Research Fellow. Since Aug. 2001, he is a senior research engineer in Institute of High Performance Computing (IHPC), A*Star, Singapore. His current research interests include fast algorithm and parallel computing techniques in computational electromagnetics, numerical simulation of complex electromagnetic materials, photonic crystals and high-speed electronic circuit package.

Alexander Bauer, born in Karlsruhe, Germany on 26 May 1980. In 2000, he was enrolled, as a Diplom (Master's degree) student, in the Department of Electrical Engineering, University of Karlsruhe, Germany. From June 2004 to November 2004, he was with the Institute of High Performance Computing, Agency for Science, Technology and Research (A*STAR), as an exchange student under National University of Singapore (NUS). His research interests focus on electromagnetics and wireless communication.

Er Ping Li received his M.Eng. from Xi'an Jiaotong University, China and Ph.D. from Sheffield Hallam University, UK both in electrical engineering in 1986 and 1992 respectively. He has been a research fellow and lecturer at Sheffield Hallam University from 1989 to 1992, senior research fellow and project manager in Singapore research institute and private company from 1993 to 1999. In April 2000, he joined Institute of high performance computing at National University of Singapore as a member of technical staff and R&D Manager. Dr. Li is a Senior Member of IEEE and an elected deputy Chairman for IEEE EMC Chapter in Singapore. His research interests include computational electromagnetics, computational nanotechnology, high-speed electronic modeling and EMC/EMI.